

# ANALYSIS OF ADSORPTION KINETICS ON ZEOLITES AT NON ISOTHERMAL CONDITIONS AND ANALYSIS OF THE KINETICS CURVES

Arkadij BEZUS, Arlette ZIKÁNOVÁ, Miloš SMUTEK and Milan KOČIŘÍK

*J. Heyrovský Institute of Physical Chemistry and Electrochemistry,  
Czechoslovak Academy of Sciences, 121 38 Prague 2*

Received May 19th, 1980

Adsorption kinetic curves were numerically simulated for the case of simultaneous mass and heat transfer. Proposed and discussed are different methods of model testing, experimental curves fitting and of evaluation of the diffusion and heat transfer coefficients from experimental kinetic curves.

General solution of the simultaneous mass and heat transfer problem given by equation (37) in our previous paper<sup>1</sup> can be presented for a non-adiabatic, non-isothermal case  $\alpha \neq 0$ ,  $\beta \neq 0$  in the form<sup>2</sup>:

$$\gamma(\tau) = 1 - \sum_{n=1}^{\infty} \frac{2 \exp(-q_n^2 \tau) [(tg q_n)^2 / (q_n)^2]}{[(tg q_n) / q_n] \{q_n^2 [(tg q_n) / q_n] + 1\} + 2/\beta + 1}. \quad (1)$$

### Numerical Simulation of the Curves

We have used the above expression for numerical simulation of the curves, determining the roots  $q_n(\alpha, \beta)$  of the transcendental equation (2) numerically by iteration.

$$q_n = \operatorname{arctg} [(\alpha - q_n^2) / (\beta q_n)]. \quad (2)$$

The iteration was stopped when two of the next following approximations of  $q_n$  differed by less than  $10^{-5}$ . In each case 20 roots were calculated.

The graphical solution of  $q_n$  for  $\alpha = 1$ ,  $\beta = 1$  is illustrated on Fig. 1. With increasing  $n$  the dependence of  $q_n$  on  $\alpha$  becomes less pronounced and its values approach the roots of the equation

$$\operatorname{tg} q_m = -q_m / \beta, \quad (3)$$

where  $m = n + 1$  since for  $\alpha = 0$  the root  $q < \pi/2$  disappears. The roots of equation (3) are published *e.g.* in Crank's monography<sup>3</sup> (on Fig. 1 they are given by points of intersection with the dashed line). For sufficiently large  $n$  finally disappears the

dependence of  $q_n$  on  $\beta$  and the  $q_n$  values converge for the isothermic case  $\beta = 0$  to  $q_m = (2m - 1) \pi/2 = (2n - 3) \pi/2$ . Using the above given formulas, the kinetic curves both in the  $\gamma$  vs  $\tau'$  coordinates (where  $\tau' = \tau(1/3 + \beta/\alpha)^{-1}$ ) and in the  $\gamma$  vs  $\ln \tau$  coordinates were calculated numerically. Influence of  $\alpha$  and  $\beta$  parameters on the shape of kinetic curves is evident from Fig. 2–8. In addition kinetic curves for adiabatic adsorption (i.e. for  $\alpha = 0$ ), calculated by means of formula (39) of our previous

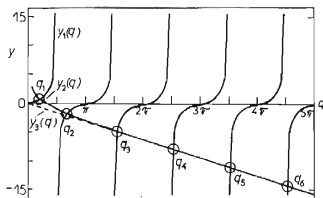


FIG. 1

Graphical Solution of Transcendental Equation  $\text{tg } q = (\alpha - q^2)/\beta q$  (the roots are given by intersections of the  $y_1(q) = \text{tg } q$ ,  $y_2(q) = (\alpha - q^2)/\beta q$ , resp.  $y_3(q) = -q/\beta$  curves)

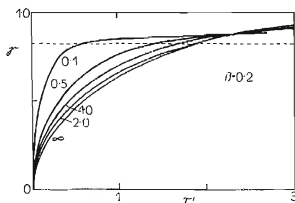


FIG. 2

Calculated Kinetic Curves in  $\gamma$  vs  $\tau'$  Coordinates for  $\beta = 0.2$  in Dependence on the  $\alpha$  Parameter (dashed line corresponds to  $\gamma = (1 + \beta)^{-1} = 0.83$ )

In Fig. 2–7 the  $\alpha$ -values are given by numbers attached to individual curves.

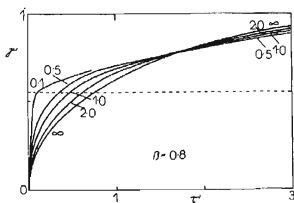


FIG. 3

Calculated Kinetic Curves in  $\gamma$  vs  $\tau'$  Coordinates in Dependence on the  $\alpha$ -Parameter (for  $\beta = 0.8$ ; dashed line:  $\gamma = 0.3$ )

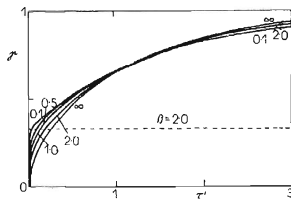


FIG. 4

Calculated Kinetic Curves in  $\gamma$  vs  $\tau'$  Coordinates in Dependence on the  $\alpha$ -Parameter (for  $\beta = 2.0$ ; dashed line:  $\gamma = 0.3$ )

paper<sup>1</sup> are given on Fig. 5–7. These curves are in very good agreement with the curves obtained by means of equation (46) of the same paper. Similarities in the shapes of adiabatic kinetic curves with different  $\beta$  parameters are evident from Fig. 9, where the curves are shown in a  $\log(\beta\gamma)$  vs  $\log(\beta^2\tau)$  plot. Individual curves can be expressed by a single master curve by simple translation along the  $\log(\beta^2\tau)$  axis and by scaling of the  $\log(\beta\gamma)$  axis. A magnitude of the translation with respect to the  $\beta = 1$  case can be read from the marked zero positions on each curve (symbol 0).

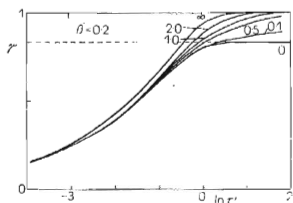


FIG. 5

Calculated Kinetic Curves in  $\gamma$  vs  $\ln \tau$  Coordinates in Dependence on the  $\alpha$ -Parameter (for  $\beta = 0.2$ ; dashed line:  $\gamma = 0.83$ )

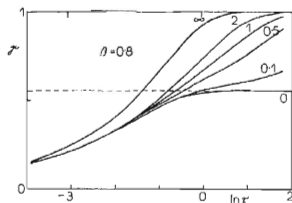


FIG. 6

Calculated Kinetic Curves in  $\gamma$  vs  $\ln \tau$  Coordinates in Dependence on the  $\alpha$ -Parameter (for  $\beta = 0.8$ ; dashed line:  $\gamma = 0.3$ )

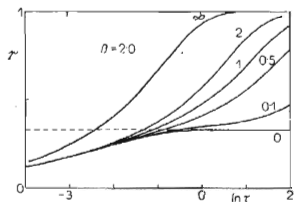


FIG. 7

Calculated Kinetic Curves in  $\gamma$  vs  $\ln \tau$  Coordinates in Dependence on the  $\alpha$ -Parameter (for  $\beta = 2.0$ ; dashed line:  $\gamma = 0.3$ )

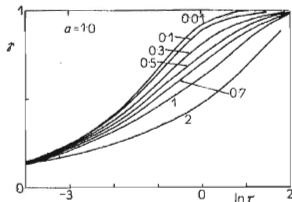


FIG. 8

Calculated Kinetic Curves in  $\gamma$  vs  $\ln \tau$  Coordinates in Dependence on the  $\beta$ -Parameter (for  $\alpha = 1$ )

We have used in this alternative method of calculation only the first three roots of the transcendental equation (3), which were determined for  $\beta \leq 2$  from the following correlations:

$$q_1^2(\beta) \approx 2.467402 + 2\beta - 0.40526\beta^2 + 0.05845\beta^3 - 0.00477\beta^4 + 0.00005\beta^5 \quad (4)$$

(max. error is found for  $\beta = 2$ , equal to  $4 \cdot 10^{-5}$ )

$$q_2^2(\beta) \approx 22.806364 + 2.25266\beta - 0.012\beta^2 - 0.02713\beta^3 + 0.00312\beta^4 \quad (5)$$

(error for  $\beta = 2$  equals  $3.7 \cdot 10^{-5}$ )

$$q_3^2(\beta) \approx 184.726234 + 16.74776\beta + 0.4155\beta^2 - 0.0293\beta^3 + 0.0009\beta^4 \quad (6)$$

(error for  $\beta = 2$  equals  $3.6 \cdot 10^{-4}$ ).

#### *Methods of Model Testing and Evaluation of Kinetic Data from the Experimental Curves*

a) *Statistical moment analysis.* Information on rate mechanism and rough estimation of kinetic parameters can be obtained by evaluation of statistical moments from the measured kinetic curves<sup>4-6</sup> in dependence on the characteristic size of the adsorbent particle. In our model of non-isothermal adsorption the following formula is valid for the first moment  $(E_\omega)_\tau$  of the non-adiabatic kinetic curve for the adsorbent in a form of an infinite plate with a thickness  $2L$ :

$$(E_\omega)_\tau = \int_0^\infty \tau(dy/d\tau)d\tau = (1/3) + (\beta/\alpha), \quad (7)$$

where the subscript  $\tau$  relates to dimensionless time.

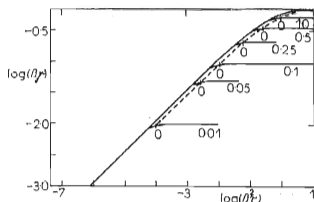


FIG. 9  
Calculated Kinetic Curves of Adiabatic Adsorption in  $\log(\beta\gamma)$  vs  $\log(\beta^2\tau)$  Coordinates in Dependence on the  $\beta$ -Parameter

For the adiabatic process we obtain:

$$(E_{\omega})_{\tau, \text{adiab}} = (1/3)(1 + \beta)^{-1}. \quad (8)$$

A relation of the above quantities to the corresponding characteristics of the experimental curves is given by equation:

$$(E_{\omega})_t = (L^2/D_{\text{eff}})(E_{\omega})_{\tau}. \quad (9)$$

Therefore for the non-adiabatic case we have a parabolic dependence on  $L^2$ :

$$(E_{\omega})_t = (L^2/D_{\text{eff}})[(1/3) + (\beta/\alpha)] = K_1 L^2 + K_2 L, \quad (10)$$

where  $K_1$  and  $K_2$  are constants.

Advantage of the statistical moment analysis lies in simplicity of the expressions. In addition, formulas often can be derived even in such cases when it is difficult to find a complete solution of the problem. Disadvantage of this method can be seen in inaccuracy of the evaluation of the moments, which can be reduced only by a very careful analysis of the kinetic curves tails. Further disadvantage can be found in the averaging of information, leading consequently to lower sensitivity towards changes in conditions of the experiment. It is *e.g.* very difficult to distinguish within the experimentally accessible range of plate thicknesses between the non-isothermal model characterized by equation (10) and the bidisperse model with a linear moment dependence on  $L^2$ :

$$(E_{\omega})_{\tau} = K_1 L^2 + K_0. \quad (11)$$

Suitability of the moment analysis has been discussed in detail in connection with thermal effects in paper<sup>7</sup>. It was found that some other kinetic effects could also lead to a parabolic dependence on  $L^2$ , *e.g.* the valve effect<sup>8,9</sup>.

The moment analysis was also applied in connection with an alternative method of kinetic data evaluation.

b) *Comparison of experimental and theoretical curves in the  $\gamma$  vs  $\tau'$  coordinates.* In this approach the first statistical moment of the experimental kinetic curve  $(E_{\omega})_{t, \text{exp}}$  is determined and the experimental kinetic curve is plotted in the  $\gamma$  vs  $t'$  coordinates, where  $t' = t/(E_{\omega})_{t, \text{exp}}$ . The  $\beta$  parameter determination must be based on independent equilibrium measurements. The experimental kinetic curves in  $\gamma$  vs  $t'$  coordinates are then compared with a set of the  $\gamma$  vs  $\tau'$  theoretical curves which are plotted for fixed  $\beta$  and different  $\alpha$  values. The  $\alpha$  parameter is estimated from the best fit of the experimental curve. By means of equations (7) and (9) we can calculate on the basis of the known values of  $(E_{\omega})_t$ ,  $\alpha$  and  $\beta$  the effective diffusion coefficient

$D_{\text{eff}}$  for isothermal diffusion. More sensitive and more accurate proved to be the next method of the experimental and theoretical curve fitting.

c) *Comparison of experimental and theoretical curves using the logarithmic plot on the time scale.* In this approach experimental curves in the  $\gamma$  vs  $\ln t$  coordinates are compared for an independently estimated  $\beta$  parameter and different  $\alpha$  values with a system of theoretical curves  $\gamma$  vs  $\ln \tau$ . On basis of a best fit achieved by translation of the curves along the  $\ln t$  axis, parameter  $\alpha$  can be estimated. The isothermal diffusion coefficient  $D_{\text{eff}}$  can thus be found from the relation:

$$\ln \tau_{\gamma} = \ln (D_{\text{eff}}/L^2) + \ln t_{\gamma}, \quad (12)$$

where  $t_{\gamma}$  and  $\tau_{\gamma}$  are time coordinates on the experimental and the theoretical curves (of determined  $\alpha$  and  $\beta$ ), corresponding to the same chosen value of  $\gamma$ .

d) *Information obtained from the end tail analysis of the kinetic curves.* The linearity of the  $\ln(1 - \gamma)$  vs  $t$  dependence at large time values was used for analysis of the thermal effects already by Ruthven<sup>10</sup>. Careful analysis of the theoretical solution shows that great care must be taken when interpreting obtained results. The analysis suggests that the discussed model of simultaneous mass and heat transfer results at sufficiently large time values always in a linear dependence of  $\ln(1 - \gamma)$  on  $t$ :

For the isothermal case  $\alpha \rightarrow \infty$  or  $\beta = 0$  we have

$$\ln(1 - \gamma) \approx \ln(8/\pi^2) - (\tau/\pi^2). \quad (13)$$

For the strongly non isothermal case ( $\alpha \leq 0.1$ ) it holds:

$$\begin{aligned} \ln(1 - \gamma) &\approx \ln[\beta/(1 + \beta)] - [\alpha(1 + \beta)]\tau = \\ &= \ln[\beta/(1 + \beta)] - ht/[L\varrho_p\kappa_p(1 + \beta)]. \end{aligned} \quad (14)$$

It is evident that in contrast with the isothermal case no information on diffusion can be drawn from the exponential shape of a curve tail since at these conditions the process is entirely limited by the rate of heat dissipation.

Combining the criteria

$$D_{\tau}/D_{\text{eff}} \geq 100 \quad (15)$$

and

$$\alpha = hL/D_{\text{eff}}\varrho_p\kappa_p \leq 0.1 \quad (16)$$

we obtain for zeolitic compacts, using for  $D_T = 6 \cdot 10^{-7} \text{ m}^2 \text{ s}^{-1}$ ,  $\rho_p = 1000 \text{ kg m}^{-3}$ ,  $\kappa_p = 0.9 \text{ J g}^{-1} \text{ K}^{-1}$  and  $h \approx 1.7 \cdot 10^{-2} \text{ kJ m}^{-2} \text{ K}^{-1} \text{ s}^{-1}$  (which is a typical value for the heat transfer coefficient we have found in our experiments):

$$L_{\max} \approx 3.2 \cdot 10^{-8} \text{ m}.$$

This value lies for zeolitic compacts close to the limits of experimental possibilities caused by low mechanical stability of the plates. Therefore this case will be of negligible significance with compacted zeolites. Nevertheless it can be shown that even for  $0.1 < \alpha < \infty$  one gets:

$$\gamma(\tau) \approx 1 - \frac{5(3\beta + \alpha) - (5 + \beta)\mu}{(6 + \beta)(\lambda - \mu)} \exp(-\mu\tau) - \frac{(5 + \beta)\lambda - 5(3\beta + \alpha)}{(6 + \beta)(\lambda - \mu)} \exp(-\tau\lambda), \quad (17)$$

where

$$\lambda + \mu = 3[5(1 + \beta) + 2\alpha]/(6 + \beta) \equiv A \quad (18)$$

$$\lambda\mu = 15\alpha/(6 + \beta) \equiv B \quad (19)$$

and therefore

$$\lambda = (1/2)(A + \sqrt{A^2 - 4B}) \quad (20)$$

$$\mu = (1/2)(A - \sqrt{A^2 - 4B}). \quad (21)$$

It is evident that the second exponential on the right side of equation (17) converges with increasing  $\tau$  very fast to zero and we get:

$$\ln(1 - \gamma) \approx \ln \{ [5(3\beta + \alpha) - (5 + \beta)\mu] / (6 + \beta)(\lambda - \mu) \} - \mu\tau. \quad (22)$$

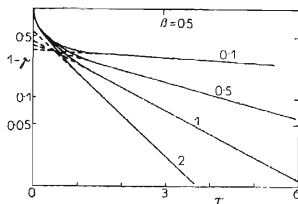


FIG. 10  
Comparison of the  $\ln(1 - \gamma)$  vs  $\tau$  Dependence Based on Exact Solution (solid line) with the Approximate Solution Based on Equation (22), (dashed line) — for  $\beta = 0.5$  and Different  $\alpha$  Values Given by Numbers Attached to Individual Curves

Fig. 10 gives a comparison of the kinetic curves approximation obtained from equation (22) with the  $\ln(1 - \gamma)$  vs  $\tau$  dependence. One can see that for  $\gamma > 0.8$  in all cases good agreement is obtained between both types of solutions. However, the approximation (22) is not very suitable for evaluation of kinetic parameters since the linear part of the dependence is not very sensitive to changes of the  $\alpha$  parameter while on the other side the slopes of the linear parts of experimental curves  $\ln(1 - \gamma)$  vs  $t$  depend on the  $\mu D_{\text{eff}}/L^2$  parameter and consequently on two kinetic quantities  $h$  and  $D_{\text{eff}}$ . The above way can be used therefore only for a model testing or for qualitative estimations of parameters.

## LIST OF SYMBOLS

$A$	abbreviation defined by equation (18)
$B$	abbreviation defined by equation (19)
$c_s'$	concentration of a sorbing compound in the crystallites (in mol/g of sorbent)
$D_{\text{eff}}$	effective diffusion coefficient
$D_T$	coefficient of thermometric conductivity ( $D_T = \lambda_p / \rho_p \alpha_p$ )
$(E_\omega)_1$	first statistical moment of the experimental curve
$(E_\omega)_\tau$	first statistical moment of the kinetic curve in dimensionless time
$h$	heat transfer coefficient on the surface of a zeolite compact
$K_0, K_1, K_2$	constants in equations (10) and (11)
$L$	half thickness of a compact
$p$	pressure of a sorbing species
$q_n$	the $n^{\text{th}}$ root of transcendental equation (2)
$q_m$	the $m^{\text{th}}$ root of transcendental equation (3)
$T$	sample temperature
$t$	time coordinate
$t'$	dimensionless time $t' = t/(E_\omega)_1$
$\tau_\gamma$	time parameter value of the experimental kinetic curve corresponding to saturation $\gamma$
$\alpha$	parameter defined by equation $\alpha = hL/D_{\text{eff}}\rho_p\alpha_p$
$\beta$	parameter defined by equation $\beta = \Delta H_{\text{ad}}(\partial c_s'/\partial T)_p/\alpha_p$
$\gamma$	relative saturation of a sorbent by a sorbing compound
$(-\Delta H_{\text{ad}})$	differential molar adsorption heat
$\alpha_p$	heat capacity of a zeolite compact
$\lambda$	parameter defined by equations (18) and (19)
$\lambda_p$	heat conductivity of a compact
$\mu$	parameter defined by equations (18) and (19)
$\rho_p$	density of a compact
$\tau = D_{\text{eff}}t/L^2$	dimensionless time parameter
$\tau' = \tau(1/3 + \beta/\alpha)^{-1}$	dimensionless time parameter
$\tau_\gamma$	value of the corresponding time parameter corresponding to $\gamma$ saturation

## Indices

$p$	relates to the zeolitic compact
$\omega$	relates to unification of all regions of different pore types which are present in a porous particle



## REFERENCES

1. Kočířik M., Smutek M., Bezus A., Zikánová A.: *This Journal* 45, 3392 (1980).
2. Zikánová A., Kočířik M., et al.: *Conference proceedings on The Properties and Applications of Zeolites* (R. P. Townsend, Ed.). London, April 1979.
3. Crank J.: *The Mathematics of Diffusion*. Clarendon Press, Oxford 1975.
4. Kočířik M., Zikánová A.: *Z. Phys. Chem. (Frankfurt am Main)* 71, 311 (1970).
5. Kočířik M., Zikánová A.: *Z. Phys. Chem. (Leipzig)* 250, 250 (1972).
6. Kärger J., Bülow M., Struve P., Kočířik M., Zikánová A.: *J. Chem. Soc., Faraday Trans. 1* 74, 1210 (1978).
7. Kočířik M., Kärger J., Zikánová A.: *J. Chem. Tech. Biotechnol.* 29, 339 (1979).
8. Kočířik M., Zikánová A.: *Ind. Eng. Chem. Fundam.* 13, 347 (1974).
9. Zikánová A., Kočířik M., Bezus A., Struve P., Hládek L.: Unpublished results.
10. Ruthven D. M.: Presented at the CHISA Conference, Prague, 1978.

Translated by Z. Dolejšek.